Nucl Eng Technol 47 (2015) 380–387

Available online at www.sciencedirect.com

ScienceDirect

journal homepage: http://www.journals.elsevier.com/nuclear-engineering-and-technology/

Technical Note

DESIGN OPTIMIZATION OF RADIATION SHIELDING STRUCTURE FOR LEAD SLOWING-DOWN SPECTROMETER SYSTEM

JEONG DONG KIM [a], *SANGJOON AHN* [a], *YONG DEOK LEE* [a], *and CHANG JE PARK* [b,*]

[a] *Nonproliferation System Research Division, Korea Atomic Energy Research Institute, Yuseong, Daejeon 305-353, Republic of Korea*
[b] *Department of Nuclear Engineering, Sejong University, Gwangjin, Seoul 143-747, Republic of Korea*

ARTICLE INFO

Article history:
Received 29 September 2014
Received in revised form
8 January 2015
Accepted 12 January 2015
Available online 4 February 2015

Keywords:
Concrete
High-density polyethylene–Borax
Isotopic assay
Lead slowing-down spectrometer facility
Radiation shielding
Spent nuclear fuel

ABSTRACT

A lead slowing-down spectrometer (LSDS) system is a promising nondestructive assay technique that enables a quantitative measurement of the isotopic contents of major fissile isotopes in spent nuclear fuel and its pyroprocessing counterparts, such as ^{235}U, ^{239}Pu, ^{241}Pu, and, potentially, minor actinides. The LSDS system currently under development at the Korea Atomic Energy Research Institute (Daejeon, Korea) is planned to utilize a high-flux ($>10^{12}$ n/cm^2·s) neutron source comprised of a high-energy (30 MeV)/high-current (~2 A) electron beam and a heavy metal target, which results in a very intense and complex radiation field for the facility, thus demanding structural shielding to guarantee the safety. Optimization of the structural shielding design was conducted using MCNPX for neutron dose rate evaluation of several representative hypothetical designs. In order to satisfy the construction cost and neutron attenuation capability of the facility, while simultaneously achieving the aimed dose rate limit (<0.06 μSv/h), a few shielding materials [high-density polyethylene (HDPE)–Borax, B_4C, and Li_2CO_3] were considered for the main neutron absorber layer, which is encapsulated within the double-sided concrete wall. The MCNP simulation indicated that HDPE-Borax is the most efficient among the aforementioned candidate materials, and the combined thickness of the shielding layers should exceed 100 cm to satisfy the dose limit on the outside surface of the shielding wall of the facility when limiting the thickness of the HDPE-Borax intermediate layer to below 5 cm. However, the shielding wall must include the instrumentation and installation holes for the LSDS system. The radiation leakage through the holes was substantially mitigated by adopting a zigzag-shape with concrete covers on both sides. The suggested optimized design of the shielding structure satisfies the dose rate limit and can be used for the construction of a facility in the near future.

* *Corresponding author.*
E-mail address: parkcj@sejong.ac.kr (C.J. Park).

http://dx.doi.org/10.1016/j.net.2015.01.004
1738-5733/Copyright © 2015, Published by Elsevier Korea LLC on behalf of Korean Nuclear Society.

1. Introduction

An accurate isotopic assay of the fissile materials in spent nuclear fuel assemblies, such as ^{235}U, ^{239}Pu, and ^{241}Pu, is key to improving the nuclear proliferation resistance of current fleets of nuclear power plants and the closed nuclear fuel cycle that can be realized in the near future. However, the International Atomic Energy Agency has determined that the current nondestructive assay methods for plutonium measurement have approximately 10% uncertainty. Lead slowing-down spectrometry (LSDS) is an active nondestructive assay method that has the potential to enable a more accurate, direct, independent, and real-time isotopic quantification of fissile materials with a considerably lower uncertainty than 10% [1].

An LSDS system is under development at the Korea Atomic Energy Research Institute (KAERI; Daejeon, Korea) for enhanced surveillance of nuclear materials and quality assurance of refabricated nuclear fuel from the back-end of the closed fuel cycle, which is in a gradually developing status in the country [2–4]. The LSDS system is planned to be comprised of a high-energy (30 MeV)/high-current (up to ~2 A) electron linear accelerator (e-LINAC) and an array of metal plates (W, Ta, or U), which is a high flux ($>10^{12}$ n/cm$^2\cdot$s) neutron source located at the center of a 1.7-m wide lead pile. The high-energy electron beam incident to the metal target produces fast neutrons through the combined (e, γ) (γ, n) reaction [5,6]. The high-purity lead stack (<5 ppmH) is employed for neutron moderation to eventually induce the fission of fissile isotopes contained in the sample, such as a spent nuclear fuel assembly or its pyro-processing counterparts, with epithermal neutrons consisting of a continuous energy spectrum in which only an insignificant portion of its constituent neutrons were moderated by light elements, e.g., hydrogen [7]. Therefore, a very intense and complex radiation field due to neutrons and γ-rays is unavoidable for an LSDS facility, and additional fast neutrons are emitted from the fission of fissile materials in the measurement area located within the lead pile. Hence, to guarantee radiation safety for the facility, the shielding structure design is a mandatory course of development of the LSDS system.

The objectives of the shielding design evaluation for the KAERI LSDS system are to select the most suitable neutron absorber among well-known materials [e.g., B_4C, Li_2CO_3, and high-density polyethylene (HDPE)–Borax] and simultaneously optimize the collective wall thickness with the selected neutron absorber layer, while achieving the radiation dose limit for nonradiation workers (<0.1 μSv/h) on the outer wall surface. The evaluation also aims to confirm the effectiveness of the elicited shielding structure design for e-LINAC instrumentation holes; both sides of the instrumentation holes for e-LINAC equipment were sheltered by extra concrete covers to achieve the radiation dose limit without remarkably increasing the shielding volume.

In this study, triple-layered structures were proposed to simultaneously shield the high-energy photons, and fast and thermal neutrons. To utilize the available facility space and construction cost efficiently, a computational optimization study on the design parameters of the shielding structure was conducted using MCNPX [8]. Further descriptions of the suggested shielding designs are specified in detail in Section 2, including the selection processes for the shielding materials and the thickness optimization for each shielding layer. The Monte Carlo simulation results are provided in Section 3. The shielding performances of the suggested shielding structures are comparatively discussed in Section 4. The last section summarizes the optimized design of the overall shielding structure for the LSDS system in KAERI.

2. Shielding design for the LSDS system facility

A systematic advantage of the LSDS system in terms of the radiation protection is the lead pile that encloses the neutron source to act as the slowing-down medium, and thus also remarkably attenuates the high energy γ-rays and moderates the neutron energy spectrum as functional byproducts. However, a complex radiation field of relatively lower energy photons and neutrons than the initially-induced radiation still requires the use of concrete as a γ-ray shield and structural material. Also, at least one additional absorber should be added for effective neutron shielding to satisfy the limit of the allowable dose rate with a minimal volume increase of the shielding structure, while ensuring its mechanical integrity. Therefore, a separate neutron absorber layer was introduced into the system owing to the concerns regarding the difficulty of a homogeneous mixing of the neutron absorber material within the concrete layer. Other important design parameters of the radiation shielding structure for the LSDS system to be determined are: (1) neutron absorber materials; (2) the relative locations of different neutron absorber layers; (3) thicknesses of all shielding layers; and (4) installation of hole structures and their locations. The following subsections are dedicated to the qualitative development of a reference shielding structure to be evaluated using the MCNPX code while varying the aforementioned design parameters within the appropriate ranges under the given circumstances.

2.1. *Shielding material selection*

Concrete is one of the most commonly used neutron absorbing materials, which consists of low Z elements and water. However, its radiation shielding capability varies with its water content. For instance, a 1% decrease in water content causes a ~60% increase in the dose rate. Thus, the loss of water after construction is a huge weakness of concrete from the standpoint of steady radiation protection. Its low density can also be another shortcoming when using only concrete, either limiting the full utilization of the facility space due to an increase in wall thickness, or imposing the use of a bulky experimental facility, which likely demands higher construction costs.

To resolve the abovementioned issues, the addition of one of several other commonly-used neutron absorbers, such as HDPE-Borax, B_4C, and Li_2CO_3, were considered. Table 1 shows the chemical compositions and densities of the candidate

materials. To be selected as the neutron shielding material for an LSDS system, a large neutron absorption cross-section is apparently the first criterion for better radiation attenuation capability.

However, a low neutron reflectivity, or low neutron scattering cross-section, is a nuclear material property of much importance in the LSDS system because neutrons reflected outside the lead pile, and therefore returned back to the system, clearly violate the correlation between the source neutron energy and slowing-down time, hence would cause large errors on the measured isotopic contents of fissile materials.

If a significant number of neutrons that have left the system reenter into the lead pile, thereby causing the fission of fissile isotopes included in the sample, fission neutron counting rates measured by the threshold fission chambers installed in the measurement area cannot be further considered as solely induced by the source neutrons, which have the same slowing-down time after their birth from the metal target. In other words, if the source neutrons inducing the fission of fissile isotopes are slowed down for different times due to the neutrons scattered back from the shielding layers, the obtained fission neutron counting rate will be intrinsically contaminated, which practically disables the calibration and therefore devalues the measured data to be almost unreliable. Consequently, the fraction of neutrons arriving at the measurement area after reentering the LSDS system should be lower than ~1% of the incident neutrons to the innermost shielding layer to maintain the measurement feasibility of the system.

Fig. 1 shows the model geometry of the shielding structure designed to compare the neutron reflectivities of all absorber materials given in Table 1. The lead pile located at the center of the geometry has a 170-cm wide cube shape and its outer surface is vertically 50 cm apart from the innermost shielding layer whose thickness is fixed at 10 cm solely for neutron reflectivity evaluation purposes. The neutron reflectivities of all candidate materials were calculated from Eq. (1) and the results of MCNP simulation using the described geometry.

$$R = \left(\frac{\Phi_2 - \Phi_1}{\Phi_1}\right) \times 100 \quad (1)$$

Table 1 – Summary of the material properties of neutron absorbing materials.

Material property	Neutron absorbing materials		
	HDPE-Borax	B_4C	Li_2CO_3
Chemical comp.(weight)			
Hydrogen	0.11		
Lithium			0.1879
Boron	0.05	0.783	
Carbon	0.6604	0.217	0.1625
Oxygen	0.1272		0.6496
Sodium	0.0522		
Density (g/cm^3)	1.1433	2.52	2.11

HDPE = high-density polyethylene.

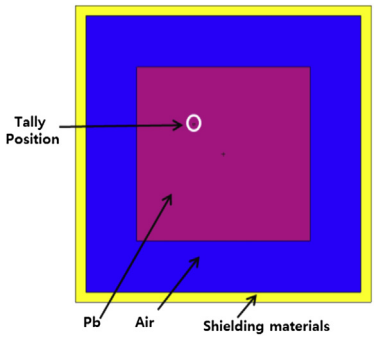

Fig. 1 – Model geometry for calculation of neutron reflectivity of shielding materials.

where R is the reflectivity and Φ_1 (or Φ_2) is the calculated average neutron flux at the tally point in the lead pile, as denoted in Fig. 1, without (or with) the shielding layer. The location of the tally point in Fig. 1 was determined by referring to the tentative location of the measurement area.

Table 2 shows the results of the MCNP simulation using a geometry that indicates that HDPE-Borax exhibited the lowest neutron reflectivity among all candidate materials and simultaneously satisfies the 1% criteria.

The radiation attenuation capability is the second-most important factor for the selection of a neutron absorber for the LSDS system. Fig. 2 shows the model geometry established for the evaluation of the radiation attenuation capabilities of the absorbers using the MCNP code. To trace the dose rate change effectively following the increase in the shielding layer thickness, the total 50 cm thick shielding layer was divided into five cells with even thicknesses of 10 cm, as shown in Fig. 2. The dimensions of the lead cube and the gap between the lead pile and the shielding layer are identical to the one shown in Fig. 1. The dose rates were directly calculated from the modified dose function built into the MCNP code and the neutron fluxes tallied at the outermost shielding layer of the model geometry.

2.2. *Shielding structure for outer wall*

As mentioned in the previous section, the radiation shielding wall consists of multiple layers of the selected radiation shielding materials, i.e., concrete and HDPE-Borax, because the two materials cannot easily be mixed homogeneously at a reasonable cost. However, due to the energy-dependent neutron cross-sections of the selected materials, it was

Table 2 – Neutron reflectivity of the shielding materials.

Shielding materials	Neutron flux (#/cm^2.s)	Reflectivity (%)
Pb	4.565E-04	
Pb + Borax	4.604E-04	0.85
Pb + B_4C	4.608E-04	0.93
Pb + Li_2CO_3	4.626E-04	1.33

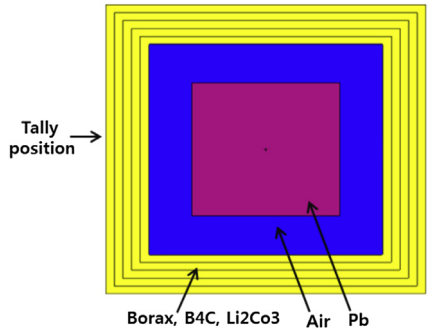

Fig. 2 – Model geometry for dose rate calculation for shielding materials.

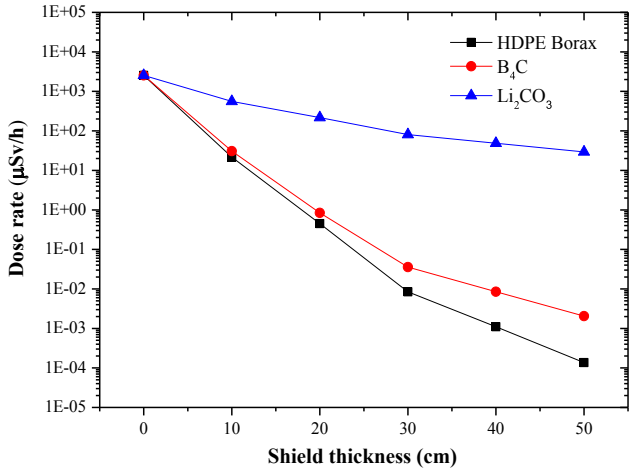

Fig. 3 – Calculated dose rates with respect to the thickness of different absorber layers.

expected that the overall performance of the shielding structure, in terms of radiation attenuation capability and neutron reflectivity, would be highly dependent on the arrangement of shielding layers, which are made of different neutron absorbers. An arrangement that minimizes the dose rate was investigated using the geometry shown in Fig. 4. In the model geometry, the lead pile dimensions and shape are maintained the same as in the above MCNP simulations (170-cm wide cube), but the lead pile and the innermost wall are separated by 100 cm (the gap is still filled with air). The total thickness of the concrete layers is maintained at 50 cm regardless of whether a single or double layer structure results from placing the 25-cm thick HDPE-Borax layer for the inside, center, or outside concrete layer(s). The dose rates were tallied at the outermost surface of the shielding structure. The results of the MCNP simulations for each case, differing only by the location of the HDPE-Borax layer with respect to the concrete layer(s), are shown in Table 3. The optimized conditions for the radiation shielding structure obtained from a comparative evaluation of the results are summarized in the following section.

2.3. *Shielding materials thickness optimization*

Since the previous subsections describe the shielding material selection and optimization of the arrangement of each shielding layer with a preview of the simulation results, the optimization of the thickness of each shielding layer can be conducted more comprehensively with the design information for the facility.

The tentative goal for the dose rate limit for the KAERI LSDS system facility is 0.06 μSv/h, which has a 40% margin from the actual limit for the dose rate (0.1 μSv/h) for nonradiation workers at a radiation facility; the margin was willfully adopted with the sole aim of ensuring the radiation safety for the facility.

Before the thickness optimization, two representative types of concrete (one heavy and the other ordinary) were considered to affirm whether the radiation shielding performance intrinsically varies significantly along with the density change. Thus, the thickness of the concrete layer was optimized for the two cases, i.e., ordinary concrete and heavy concrete. It was revealed as expected that heavy concrete exhibited superior radiation shielding performance, mainly due to its higher density. Therefore, heavy concrete was used for the evaluation of the dose rate at the outside of the shielding structure and for the optimization of the HDPE-Borax layer thickness.

With the optimized HDPE-Borax layer thickness, MCNP simulations on the various thicknesses of the inner and outer heavy concrete layers shown in Table 4 were conducted to find the minimum combined thickness of the layers satisfying the tentative dose rate limit (<0.06 μSv/h).

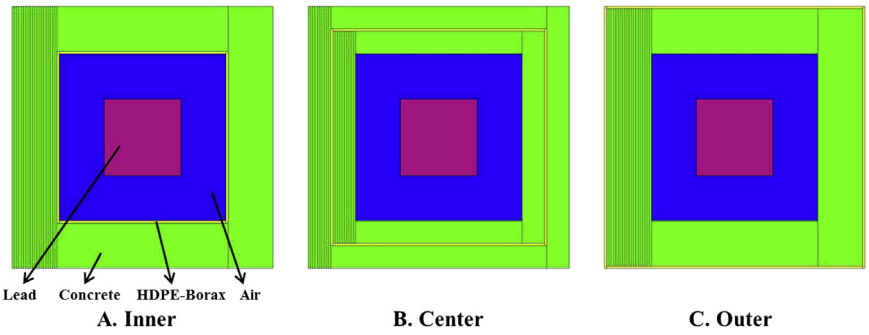

Fig. 4 – Model geometries for different arrangements of high-density polyethylene–Borax layer.

Table 3 – Dose rates for the HDPE-Borax layer arrangements.

Shielding material position	Thickness (cm)		Dose rate (μSv/h)
	Concrete	HDPE-Borax	
Inner	100	5	9.80E-01 (0.0315[a])
Center	50, 50	5	1.99E-01 (0.0249)
Outer	100	5	3.28E-01 (0.0785)

HDPE = high-density polyethylene.
[a] Fractional standard deviation (= relative error).

Fig. 5 shows the practical dimensions of the LSDS system facility under construction at KAERI. The performance evaluation of the optimized shielding structure for the ideal geometry was repeated for a practical geometry with the same selected shielding materials, shielding structure, and layer thicknesses to confirm whether the optimization based on the hypothetical geometry with a higher symmetry is still effective for the actual facility.

2.4. *Hole structure and its position*

Electrical connections and ventilation ducts should penetrate through the shielding structure since the e-LINAC equipment should be installed near the neutron target located at the center of the 170 cm wide lead cube, while the operational devices for the e-LINAC are required to be outside the radiation shielding structure.

Even when considering a single straight hole with a 5 cm diameter (considerably minimum dimension for electrical wiring) on the shielding structure, the dose rate limit was exceeded by the estimated dose rate near the hole. To match the dose rate limit with the hole structure in the shielding wall, four different positions for a hole of three different structures were considered for the evaluation of the dose rate as shown in Fig. 6.

3. Results and discussion

The performance of the shielding materials and the structure of the shielding layers of different shielding materials were evaluated for the ideal geometry to effectively shield the neutrons and high-energy γ-rays generated by the LSDS system. Based on the performance evaluations, the thickness of each shielding layer was minimized to a level barely withstanding the tentative dose rate limit, which has a 40% margin from the dose rate limit for nonradiation workers at a radiation facility.

By utilizing the results of the serial evaluation and optimization, the optimal conditions for the radiation shielding structure for the LSDS system were obtained from MCNP simulations adopting the actual geometry of the facility. In addition, the location and structure of a penetrating hole required for interconnecting the e-LINAC installed in the radiation environment and the corresponding operational devices located outside the shielding structure were selected.

For the selection of the shielding material, both the reflected neutron fraction and the outer surface dose rate of the shielding structure were compared for several common neutron absorbers.

Table 2 shows the neutron reflectivities of the considered shielding materials at a location 50 cm away from the lead pile. The calculated neutron reflectivities of the candidates are 0.85% for HDPE-Borax, 0.93% for B_4C, and 1.33% for Li_2O_3, and thus HDPE-Borax is regarded as the most suitable shielding material as an additive to heavy concrete in terms of neutron reflectivity.

Fig. 3 shows the evaluation results of the dose rates for the thickness increase of the shielding materials; all dose rates were tallied at the outer surface of the shielding structure.

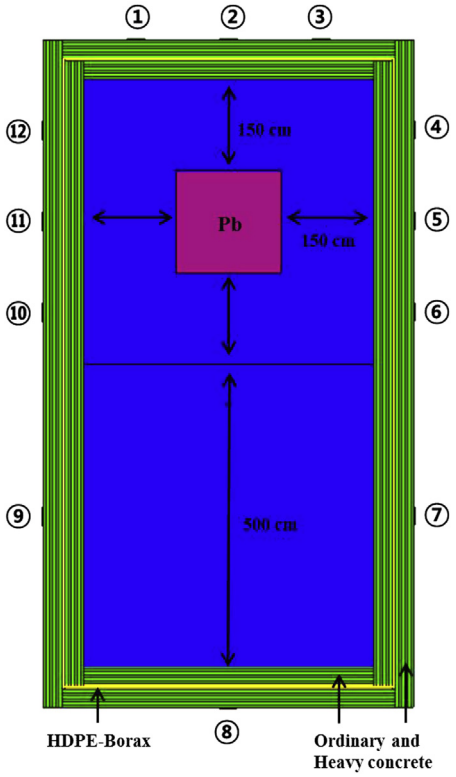

Fig. 5 – Actual geometry of Korea Atomic Energy Research Institute lead slowing-down spectrometer system facility.

Table 4 – Dose rates for varying thicknesses of ordinary and heavy concrete layers.

Ordinary concrete thickness (cm)	Dose rate (μSv/h)	Heavy concrete thickness (cm)	Dose rate (μSv/h)
137	1.19E-01 (0.03[a])	50	3.09E-00 (0.047)
138	1.09E-01 (0.035)	55	9.76E-01 (0.084)
139	9.71E-02 (0.033)	60	3.40E-01 (0.015)
140	9.05E-02 (0.036)	65	1.19E-01 (0.018)
145	5.14E-02 (0.043)	70	4.28E-02 (0.023)
150	3.05E-02 (0.058)	75	1.38E-02 (0.028)

[a] Fractional standard deviation (= relative error).

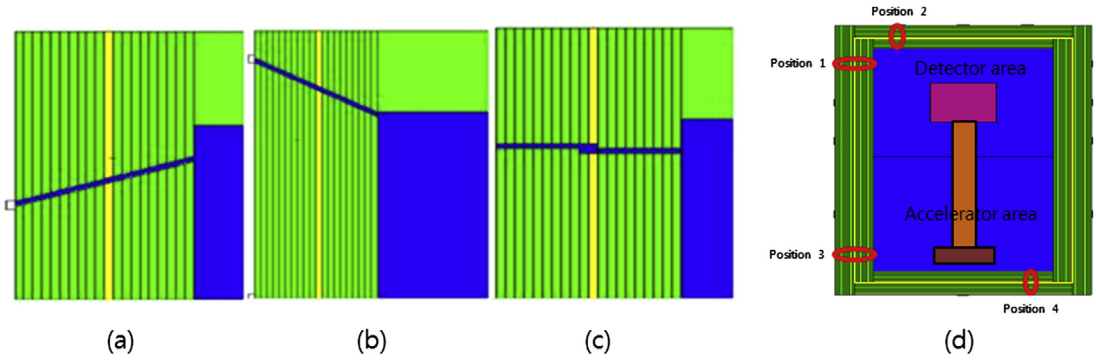

Fig. 6 – Suggested hole structures and locations.

The dose rates for B_4C and HDPE-Borax layers are comparable to each other when the layers are 10 cm thick. However, for the case of 50 cm thick layers for both materials, the estimated dose rate for the HDPE-Borax layer is approximately 10-fold lower than that for B_4C. Li_2CO_3 showed a relatively higher dose rate in general in comparison to the other two candidates.

Conclusively, the overall performance of HDPE-Borax, as the shielding material for the LSDS system in combination with heavy concrete, was revealed to be outstanding among the considered materials under the given circumstances.

The optimal arrangement of the shielding layers of concrete and HDPE-Borax were determined by the evaluation of the dose rates of the facility when varying the relative positions of the shielding layers. Fig. 4 shows the three possible arrangements of the shielding layers, which places the HDPE-Borax layer at the innermost, intermediate, and outermost locations. Table 3 shows the resulting dose rates when varying the shielding layer arrangements. Following the position of the HDPE-Borax layer, the dose rate was varied from 9.08E-01 μSv/h (innermost) to 3.28E-01 μSv/h (outermost) and finally to 1.99E-01 μSv/h (intermediate). Thus, a triple layer structure (concrete-HDPE-Borax-concrete) was determined as the optimal arrangement according to the dose rate evaluation. In other words, the MCNP simulations indicated that the HDPE layer should be sandwiched to maximize the overall performance of the radiation shielding structure.

The thicknesses of the shielding layers of the triple-layered structure were minimized based on the dose rate evaluation, fulfilling the tentative dose rate limit. Table 4 shows the dose rates changes according to layer thickness when using a single layer of concrete; the dose rate limit can be satisfied with either ordinary 145-cm-thick concrete or heavy 70-cm-thick concrete, which indicates that the use of heavy concrete enables a 75-cm-decrease of the thickness of the shielding structure.

Table 5 shows the dose rates estimated when varying the thickness of the HDPE-Borax-layer from 4 cm to 10 cm in order to determine the optimal thickness of the layer. With a 6-cm decrease of the HDPE-Borax layer thickness, the heavy concrete layer needs to be increased by 10 cm from an initial thickness of 50 cm. In addition, the HDPE-Borax layer ought to be at least 5 cm thick to fulfill the dose rate limit; in this case, the collective thickness of the shielding structure becomes 65 cm.

Table 6 shows the dose rates estimated for the various thicknesses of the ordinary concrete layer with the predetermined thickness of the HDPE-Borax layer; the dose rate limit is satisfied except in Cases 1 and 2. Thus, the optimized layer thickness of the triple-layer structure using ordinary concrete is 95 cm (45 cm–5 cm–45 cm for concrete–HDPE-Borax–concrete, respectively). In addition, it should be noted from Table 6 that increasing the thickness of the inner wall is more effective than increasing that of

Table 5 – Dose rates for varying thicknesses of high-density polyethylene-Borax.

Thickness (cm)			Dose rate (μSv/h)
Inner	Center	Outer	
25	10	25	6.79E-02 (0.03[a])
30	9	25	3.44E-02 (0.038)
30	8	25	5.08E-02 (0.039)
30	7	25	8.01E-02 (0.030)
30	6	30	3.74E-02 (0.036)
30	5	30	5.73E-02 (0.029)
30	4	30	9.18E-02 (0.026)

[a] Fractional standard deviation (= relative error).

Table 6 – Dose rates for varying thicknesses of ordinary concrete layers with 5-cm-thick high-density polyethylene-Borax layer.

Thickness (cm)				Shielding outer wall
Case	Inner	HDPE-Borax	Outer	Dose rate (μSv/h)
1	40	5	45	1.04E-01 (0.0047[a])
2	45	5	40	6.00E-02 (0.0079)
3	45	5	45	3.50E-02 (0.0101)
4	45	5	50	2.06E-02 (0.0065)
5	50	5	45	1.16E-02 (0.0135)
6	50	5	50	6.82E-03 (0.0114)

HDPE = high-density polyethylene.
[a] Fractional standard deviation (= relative error).

Table 7 – Dose rates for ordinary and heavy concrete layers estimated for the actual dimensions of lead slowing-down spectrometer system facility.

Measuring location	Ordinary concrete dose rate (μSv/h)			Heavy concrete dose rate (μSv/h)		
	Inner 50 cm Borax 5 cm Outer 45 cm	Inner 45 cm Borax 5 cm Outer 45 cm	Inner 45 cm Borax 5 cm Outer 50 cm	Inner 35 cm Borax 5 cm Outer 30 cm	Inner 30 cm Borax 5 cm Outer 30 cm	Inner 30 cm Borax 5 cm Outer 35 cm
①	1.47E-02 (0.0362[a])	4.11E-02 (0.0103)	2.531E-02 (0.0083)	1.39E-02 (0.035)	3.92E-02 (0.0309)	1.42E-02 (0.0368)
②	4.43E-02 (0.0083)	1.24E-01 (0.0069)	7.610E-02 (0.0138)	5.21E-02 (0.0234)	1.41E-01 (0.0203)	5.17E-02 (0.0212)
③	1.45E-02 (0.0142)	4.07E-02 (0.0080)	2.51E-02 (0.0083)	1.28E-02 (0.0317)	3.72E-02 (0.0321)	1.30E-02 (0.0346)
④	1.48E-02 (0.0234)	4.12E-02 (0.0094)	2.58E-02 (0.0141)	1.27E-02 (0.0303)	3.80E-02 (0.0285)	1.36E-02 (0.0323)
⑤	4.38E-02 (0.0101)	1.22E-01 (0.0053)	7.49E-02 (0.0055)	5.00E-02 (0.0196)	1.45E-01 (0.0181)	5.23E-02 (0.0212)
⑥	1.31E-02 (0.0101)	3.78E-02 (0.0084)	2.35E-02 (0.0080)	1.26E-02 (0.0319)	3.49E-02 (0.0272)	1.28E-02 (0.0293)
⑦	2.21E-03 (0.0228)	6.42E-03 (0.0236)	3.97E-03 (0.0168)	1.23E-03 (0.0965)	3.40E-03 (0.0706)	1.30E-03 (0.1087)
⑧	4.86E-03 (0.0312)	1.32E-02 (0.0190)	8.18E-03 (0.0157)	5.67E-03 (0.0842)	1.38E-02 (0.0521)	5.14E-03 (0.0655)
⑨	2.31E-03 (0.0227)	6.90E-03 (0.0276)	4.20E-03 (0.0169)	1.31E-03 (0.1013)	4.18E-03 (0.0753)	1.40E-03 (0.0896)
⑩	1.33E-02 (0.0100)	3.82E-02 (0.0100)	2.36E-02 (0.0082)	1.24E-02 (0.0322)	3.75E-02 (0.0287)	1.25E-02 (0.0286)
⑪	4.38E-02 (0.0107)	1.22E-01 (0.0062)	7.51E-02 (0.0066)	5.26E-02 (0.0219)	1.46E-01 (0.02)	5.36E-02 (0.0235)
⑫	1.44E-02 (0.0131)	4.15E-02 (0.0131)	2.58E-02 (0.0088)	1.30E-02 (0.0321)	3.75E-02 (0.0281)	1.34E-02 (0.0336)

[a] Fractional standard deviation (= relative error).

Table 8 – Dose rates varying with different structures and positions of a penetrating hole.

Shielding material	Hole Structure	Dose rate (μSv/h)			
		Position 1	Position 2	Position 3	Position 4
Concrete	Zigzag	1.22E+01 (0.101[a])	6.72E+00 (0.0738)	3.26E+00 (0.2177)	1.27E+01 (0.0816)
	Down diagonal	1.04E+02 (0.1582)	1.10E+02 (0.1403)	1.85E+01 (0.1572)	3.56E+01 (0.133)
	Up diagonal	5.49E+01 (0.0553)	5.11E+01 (0.0831)	3.00E+01 (0.5602)	4.45E+01 (0.0781)
Heavy concrete	Zigzag	1.99E+01 (0.1225)	1.13E+01 (0.0806)	4.36E+00 (0.1963)	2.41E+01 (0.048)
	Down diagonal	8.45E+01 (0.1625)	8.90E+01 (0.1789)	3.16E+01 (0.3561)	4.21E+01 (0.3979)
	Up diagonal	1.13E+02 (0.0914)	8.54E+01 (0.0709)	1.40E+01 (0.1978)	2.93E+01 (0.1127)

[a] Fractional standard deviation (= relative error).

the outer wall to diminish the dose rate at the same overall thickness of the shielding structure. For instance, dose rates for Cases 1 and 2 are 1.04E-01 μSv/h and 6.00E-02 μSv/h, respectively; about a two-fold increase in the dose rate results for Case 1 merely from moving a 5-cm-thick concrete layer from the inner to the outer wall. A similar tendency can also be confirmed from Cases 4 and 5. Hence, increasing the inner wall thickness can be concluded as more efficient than increasing the outer wall thickness to improve the radiation shielding capability of the shielding structure. However, it is likely that this tendency may only be effective for small perturbations, perhaps 5–10% based on the optimized concrete layer thicknesses.

Table 7 shows the results of the dose rate evaluation based on the actual geometry of the LSDS facility with predetermined shielding materials, layer arrangement, and the optimized layer thickness. The dose rates slightly exceed the dose rate limit at the three locations nearest to the lead pile, denoted as 2, 5, and 11. To reduce the dose rates below the limit, the thickness of either the inner or outer concrete wall was increased by 5 cm. Although the dose rates were successfully decreased below the limit in both cases, the increased inner wall yielded lower dose rates for all cases. The finalized layer dimensions of the shielding structure are 50 cm × 5 cm × 45 cm for ordinary concrete and 35 cm × 5 cm × 30 cm for heavy concrete.

Finally, the dose rate evaluation was performed on the shielding structure with various structures and locations of the penetrating hole; Table 8 shows the simulated dose rates for these cases. The dose rates were relatively lower in the cases of zigzag holes and higher when closer to the neutron source, or lead pile; however, in all cases the dose rates exceed the dose late limit. Fig. 7 shows an additional

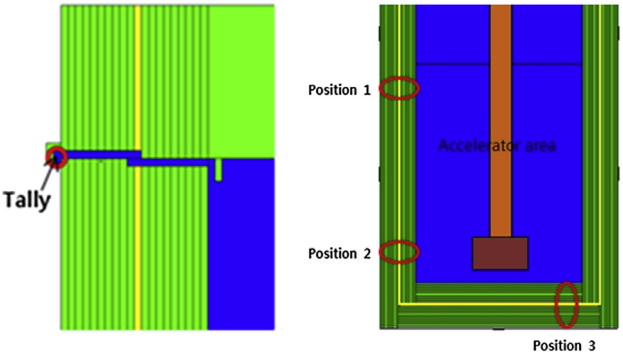

Fig. 7 – Modified hole structure and locations.

Table 9 – Dose rates at hole positions with additional concrete cover.

Cover material	Dose rate (μSv/h)		
	Position 1.	Position 2.	Position 3.
Ordinary concrete	3.57E-02 (0.031[a])	1.89E-02 (0.031)	1.99E-02 (0.029)
Heavy concrete	1.59E-02 (0.0387)	6.85E-03 (0.0401)	7.16E-03 (0.0465)

[a] Fractional standard deviation (= relative error).

5-cm-thick concrete cover located in front of the hole introduced to compensate for the hole effect, which effectively blocks the direct leakage of radiation. Table 9 shows that the dose rates for the selected zigzag hole structure combined with the additional concrete cover are below the dose rate limit.

4. Conclusion

The KAERI LSDS system can enable a more accurate and isotopic quantification of fissile isotopes in spent nuclear fuel by utilizing a high-flux ($>10^{12}$ n/cm^2·s) neutron source, which induces a very intense and complex radiation field for the facility, thus demanding structural shielding for radiation protection. Optimization of the structural shielding design was conducted using MCNPX by evaluating the neutron dose rates for several representative hypothetical designs. From the Monte Carlo code simulation, HDPE-Borax was selected owing to its outstanding performance in terms of lower neutron reflectivity and superior radiation shielding capability compared to B_4C and Li_2CO_3. The HDPE-Borax layer was determined to be encapsulated by concrete layers, which collectively form a 100-cm thick triple-layered shielding structure, comprised of a 50-cm thick inner concrete layer, a 5-cm thick intermediate HDPE-Borax layer, and a 45-cm thick outer concrete layer. The issue of a locally high dose rate near the penetrating hole on the shielding structure for the e-LINAC instrumentation needs was successfully resolved by adopting a zigzag-shaped hole and an additional 5-cm thick concrete cover. The optimized shielding structure design in this study can be referred to as the reference of importance for future LSDS system facility construction to secure radiation safety.

Conflicts of interest

All contributing authors declare no conflicts of interest.

Acknowledgments

This work was supported by the Nuclear Research Foundation of Korea (NRF) grant funded by the Ministry of Science, ICT and future Planning (MSIP) of Korea under Project (No. 2014030151).

REFERENCES

[1] J. Kulisek, K. Anderson, S. Bowyer, A.M. Casella, C. Gesh, G. Warren, Lead slowing-down Spectrometry Time Spectral Analysis for Spent Fuel Assay: FY11 Status Report, Pacific Northwest National Laboratory, 2011.
[2] Y.D. Lee, C.J. Park, J.H. Song, K.C. Song, Development of LSDS spectrometer for nuclear fissile assay, in: Global 2009, Paris, France, Sept 7–10, 2009.
[3] Y.D. Lee, C.J. Park, G.I. Park, K.C. Song, Design of lead slowing down spectrometer for spent fuel fissile assay, in: 52nd INMM, Palm Desert, California, 2011.
[4] Y.D. Lee, C.J. Park, H.D. Kim, K.C. Song, Design of LSDS for isotopic fissile assay is spent fuel, Nucl. Eng. Technol. 45 (2013) 921–928.
[5] N. Baltateanu, M. Jurba, V. Calian, G. Stoenescu, Optimal fast neutron sources using linear electron accelerators, in: Proceedings of EPAC 2000, Vienna, Austria, 2000.
[6] H.R. Radulescu, N.M. Abdurrahman, A.I. Hawari, B.W. Wehring, Pulsed neutron generator facility for slowing down time spectrometry, in: ANRCP-1999-29, Texas at Austin, 1999.
[7] H. Krinninger, E. Ruppert, H. Siefkes, Operational experience with the automatic lead-spectrometer facility for nuclear safeguards, Nucl. Instrum. Methods 117 (1974) 61–84.
[8] D.B. Pelowitz, MCNPX User's Manual, LA-CP-05–0369, Los Alamos National Laboratory, 2005.